Cement and Concrete Composites 69 (2016) 38–48

Contents lists available at ScienceDirect

Cement and Concrete Composites

journal homepage: www.elsevier.com/locate/cemconcomp

Numerical simulation of heat and mass transport during hydration of Portland cement mortar in semi-adiabatic and steam curing conditions

E. Hernandez-Bautista [a, b, *], D.P. Bentz [b], S. Sandoval-Torres [a], P.F. de J. Cano-Barrita [a]

[a] Instituto Politécnico Nacional/CIIDIR Unidad Oaxaca, Hornos 1003, Oaxaca, 71230, Mexico
[b] National Institute of Standards and Technology, Gaithersburg, MD, USA

ARTICLE INFO

Article history:
Received 18 February 2015
Received in revised form
27 May 2015
Accepted 7 October 2015
Available online 22 October 2015

Keywords:
Accelerated curing
Cement-based materials
Moisture distribution
Exothermic reaction
Isothermal calorimetry
Nuclear magnetic resonance

ABSTRACT

A model that describes hydration and heat-mass transport in Portland cement mortar during steam curing was developed. The hydration reactions are described by a maturity function that uses the equivalent age concept, coupled to a heat and mass balance. The thermal conductivity and specific heat of mortar with water-to-cement mass ratio of 0.30 was measured during hydration, using the Transient Plane Source method. The parameters for the maturity equation and the activation energy were obtained by isothermal calorimetry at 23 °C and 38 °C. Steam curing and semi-adiabatic experiments were carried out to obtain the temperature evolution and moisture profiles were assessed by magnetic resonance imaging. Three specimen geometries were simulated and the results were compared with experimental data. Comparisons of temperature had maximum residuals of 2.5 °C and 5 °C for semi-adiabatic and steam curing conditions, respectively. The model correctly predicts the evaporable water distribution obtained by magnetic resonance imaging.

1. Introduction

Steam curing of hydraulic concrete in the precast industry has the advantage of accelerating the hydration reactions of cement. Consequently, the material develops compressive strength and reduces its permeability in hours, compared to standard curing under normal environmental conditions, where the hydration reactions may require several days or even months to reach an adequate level [1].

The process of steam curing consists of increasing the temperature within a saturated water vapor atmosphere. In this process, the cement hydration has a significant impact on the temperature development inside the material at early ages [2] and also affects the mechanical and durability properties of the hardened material. Therefore, it is essential to take into account the hydration properties and temperature development to prevent premature damage to concrete.

Studies related to steam curing of concrete have been oriented toward the development of compressive strength [3–6], pore structure development [7–9] and energetic efficiency of this process [5,10].

In order to understand the mechanisms of heat and mass transport coupled with cement hydration, various models have been developed to explain these phenomena [11–17]. However, these are typically for ambient environmental conditions, therefore it is necessary to focus on hydration at elevated temperatures and high relative humidity encountered in steam curing. Additionally, the calculated degree of hydration varies with temperature during the curing cycle. This is of interest to the precast industry. With the aims of improving curing schedules, establishing appropriate curing conditions, improving mechanical properties and durability of cement-based materials and obtaining a better energy efficiency in the process, this paper investigates the numerical simulation of this curing process.

Specifically, the aim of this work is to model the hydration, moisture distribution and heat transport during the semi-adiabatic curing of cement paste and mortar specimens so that pre-cast operations can be optimized with respect to curing (cycle) time and energy efficiency. Nuclear magnetic resonance (NMR) and magnetic resonance imaging (MRI) measurements are performed to nondestructively obtain experimental evidence of the moisture distribution in small mortar specimens to validate the model predictions.

* Corresponding author. Instituto Politécnico Nacional/CIIDIR Unidad Oaxaca, Hornos 1003, Oaxaca, 71230, Mexico.
E-mail address: ehernandezb0800@alumno.ipn.mx (E. Hernandez-Bautista).

http://dx.doi.org/10.1016/j.cemconcomp.2015.10.014
0958-9465/

Nomenclature

A	Parameter for vapor diffusion coefficient kg/(m s)
b	Parameter for the liquid diffusion coefficient
c	Parameter for the liquid diffusion coefficient
C_p^{CemBM}	Cement-based material specific heat capacity J/(kg K)
C_{pi}	Specific heat capacity of the material i J/(kg K)
D_l	Liquid moisture diffusion coefficient m^2/s
D_v	Vapor diffusion coefficient kg/(m s)
$\boldsymbol{E}$	Activation energy J/mol
H	Total enthalpy of hydration J/kg
H_u	Ultimate enthalpy of hydration J/kg
h_c	Convective heat transfer coefficient W/(m^2 K)
h_m	Mass transfer coefficient g/(m^2 h Pa) or s/m
i	type of Material
k_l	Hashin–Shtrikman lower bound for the thermal conductivity W/(m K)
k_h	Hashin–Shtrikman upper bound for the thermal conductivity W/(m K)
k_1	Thermal conductivity of cement powder W/(m K)
k_2	Thermal conductivity of silica sand W/(m K)
k_i	Thermal conductivity of material i W/(m K)
M_f^{water}	Water mass fraction
$M_f^{Bondwater}$	Bound water mass fraction
M_f^{cem}	Cement mass fraction
$M_f^{silicasand}$	Aggregate mass fraction
$\vec{\mathbf{n}}$	Normal vector
P_{vext}	Vapor pressure in the surroundings Pa
P_v	Vapor pressure inside the material Pa
$\boldsymbol{Q}$	Heat generation rate W/m^3
R	Ideal gas constant J/(mol K)
S	Evaporable water sink kg/(m^3 s)
S_p	Surface of the pore system m^2
t	Time s
T_r	Reference temperature K
T	Temperature K
t_e	Equivalent time
T_2	transverse relaxation time (s)
x_1	Volume fraction of cement powder in the mix
x_2	Volume fraction of silica sand in the mix
V_p	Volume of the pore system m^3
W	Moisture content

Greek symbols

α	Degree of hydration
α_u	Ultimate degree of hydration
β	Maturity equation parameter
λ_{vap}	Heat of vaporization J/kg
ρ_i	Density of material i kg/m^3
ρ_s	Density of the solid cement-based material kg/m^3
ρ_2	Surface relaxivity m/s
τ	Maturity equation parameter s
Ω	Domain

2. Experimental procedures

2.1. Materials

The cement used in the mortar specimens was a Mexican cement designated as CPO30RS. The oxide composition measured by X-ray fluorescence is shown in Table 1. The corresponding potential Bogue phase composition, heat of hydration and water necessary for cement hydration were calculated. The latter two sets of values were obtained by multiplying the Bogue mass fractions by the accepted value for each phase as taken from the literature.

The cement density and its particle size distribution (PSD) via laser diffraction were measured at the National Institute of Standards and Technology (NIST). A density of 3150 kg/m^3 ± 10 kg/m^3 was obtained using the ASTM C188 test method [18] and the measured PSD is given in Fig. 1.

The mortar mixture proportions used in this study are provided in Table 2. Silica sand with a fineness modulus of 2.9 was used as fine aggregate. The cement, water and silica sand were mixed according to the ASTM C305-06 standard [19].

Table 1
Oxides and potential Bogue phase composition of Mexican cement CPO30RS.

Oxide	% Mass	Phase % mass	
CaO	62.5	C_3S	0.553
SiO2	21.5	C_2S	0.200
Al2O3	4.5	C_3A	0.089
MgO	2.5	C_4AF	0.055
TiO2	2.0	Heat of hydration, H_u (J/g cement) [20]	
Fe2O3	1.8	C_3S contribution	286.
Mn2O3	1.5	C_2S contribution	52.4
K2O	1.5	C_3A contribution	101.6
SO3	1.0	C_4AF contribution	39.7
Na2O	0.7	Water necessary for hydration (g/g cement) [21]	
P2O5	0.5	C_3S contribution	0.133
Total	100	C_2S contribution	0.042
		C_3A contribution	0.036
Density	3150 kg/m^3	C_4AF contribution	0.020

2.2. Method

2.2.1. Thermal property changes during cement hydration

2.2.1.1. Heat capacity. The Transient Plane Source (TPS) method uses a sensor that consists of a combined heat source and a resistance thermometer [22]. A constant power is supplied to the sensor for a specified period of time and the temperature is continuously measured. The thermal properties of the sample are calculated by analyzing the temperature development in the sensor.

For cement and dry silica sand, the heat capacity was measured using a Hot Disk Thermal Constant Analyzer with a heat capacity

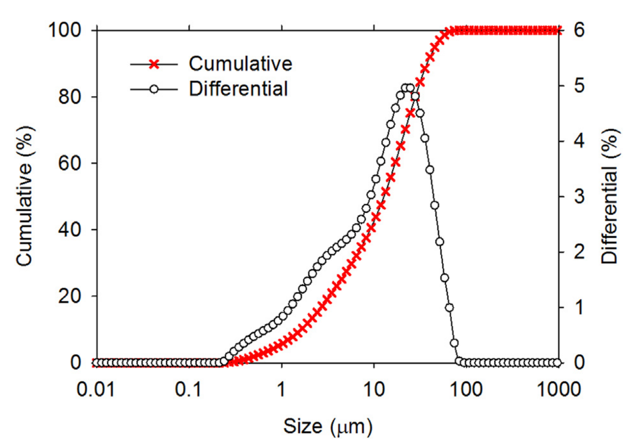

Fig. 1. Cumulative and differential PSD of the cement CPO30RS.